

Structural and optical properties of TiO₂ thin films grown by sol-gel dip coating process

Y. BOUACHIBA^{1*}, A. BOUABELLOU¹, F. HANINI¹, F. KERMICHE¹,
A. TAABOUCHE¹, K. BOUKHEDDADEN²

¹Laboratoire Couches Minces et Interfaces, Université Constantine 1, Constantine 25000, Algérie

²Groupe d'Etude de la Matière Condensée, CNRS-Université de Versailles/St. Quentin en Yvelines,
45 Avenue des Etats Unis F78035 Versailles Cedex, France

The mono and bi-layer TiO₂ thin films have been prepared by sol-gel method on glass. X-Ray diffraction, Raman spectroscopy, atomic force microscopy, spectroscopic ellipsometry and m-lines spectroscopy techniques have been used to characterize the TiO₂ films. The mono-layer film is found to be amorphous, while the bi-layer film shows the presence of anatase phase. The bi-layer film exhibits more homogeneous surface with less roughness. The thickness effect on the refractive index, extinction coefficient, packing density and optical band gap is analysed. The waveguiding measurements of the bi-layer film exhibit single-guided TE₀ and TM₀ polarized modes from which we can measure the refractive index and the film thickness.

Keywords: *TiO₂; anatase; AFM; ellipsometry; m-lines*

© Wrocław University of Technology.

1. Introduction

Titanium oxide (TiO₂) thin films are of significance in many industrial applications such as photocatalysts [1], sensors [2], electrochromic displays [3], solar cells [4], antireflection films [5] and optoelectronic materials [6]. For optoelectronic and optical applications it is important to know the optical properties of thin films, especially the refractive index and the extinction coefficient.

At atmospheric pressure TiO₂ exists in three crystalline phases which are rutile, anatase and brookite. In addition to the fully crystalline phase, partially crystalline or non-crystalline TiO₂ is frequently encountered especially in thin films. These materials can be classified in terms of decreasing nearest neighbor atomic order as nanocrystalline or amorphous. In a number of applications, nanocrystalline anatase is technologically the preferred form of TiO₂ [7].

Different methods have been used to prepare TiO₂ films: hydrothermal method [8],

radio frequency sputtering [9], pulsed laser deposition [10], and sol-gel methods [11, 12]. The sol-gel process, as a very promising technique, has gained particular attention. This technique is characterized by its low processing cost, its simplicity and ability to produce thin and uniform films on large substrate area, using organic and inorganic precursors. In particular, the sol-gel processes are efficient in producing thin, transparent, multi component oxide layers of many compositions on various substrates, including glass.

For an accurate measurement of optical constants and thickness, many attempts and theories were established. Among them, the m-lines spectroscopy and the spectroscopic ellipsometry have been found favorable for characterization of thin solid films, especially the semiconductors. These techniques are of high sensitivity, high accuracy, and are able to easily measure optical constants and thickness.

In this study, spectroscopic ellipsometry was used to determine the refractive index and the extinction coefficient of TiO₂ thin films.

*E-mail: physique99@gmail.com

Optical properties of materials are described by refractive index $n(\lambda)$ and extinction coefficient $k(\lambda)$ that comprises the complex index of refraction. Consequently, two sets of refractive indices and extinction coefficients are required to fully describe optical properties of anatase at each wavelength. The m-lines spectroscopy was used to determine the refractive index and thickness simultaneously. The results were correlated with structural properties.

The main objective of this work is to establish the best synthesis conditions of TiO₂ sol-gel films and show the possibility of elaboration of TiO₂ films with the structures varying from amorphous to containing mainly anatase, in order to obtain high quality transparent thin films for optoelectronic and optical applications.

2. Experimental

The TiO₂ thin films were prepared by the sol-gel process which is based on the hydrolysis of alkoxydes in alcoholic solutions in the presence of an acid catalyst. The procedure of preparation included the dissolution of titanium isopropoxide in isopropanol alcohol. The solution was left under closed stirring for 10 minutes. Then, acetic acid was poured under stirring for the following 15 minutes. Finally, methanol was added and stirred for 2 hours. The obtained solution was transparent, of yellowish color. The ordinary glass substrates (refractive index 1.517), carefully cleaned were dipped into the solution and then pulled up at a constant rate of 10 cm/min. After each dipping, the thin films were dried for 15 min. Finally, the mono-layer and bi-layer TiO₂ thin films were annealed at 500 °C for 2 hours.

X-Ray diffraction (XRD) patterns were recorded on Siemens D8 diffractometer using copper $K\alpha$ radiation. The Raman spectra were recorded at room temperature with Renishaw inVia Raman microanalytical spectrometer equipped with a motorized x-y stage and autofocus. The observation of surface morphology of TiO₂ films in a region of $10.14 \times 10.14 \mu\text{m}^2$ area was carried out using an atomic force microscopy (AFM) (Pacific Nanotechnology) operating in contact

mode. The spectroscopic measurements (SE) were performed on Horiba J. Y. Ellipsometer UVISEL. The waveguiding measurements were carried out by Metricon m-lines spectroscopy (the model 2010/M prism coupler). A right-angle rutile prism P₂ ($n_{TE} = 2.8639$, $n_{TM} = 2.5822$) was used for coupling light of a He-Ne laser with a wavelength of $\lambda = 632.8$ nm into the waveguide.

3. Results and discussion

3.1. Structural properties

XRD patterns of TiO₂ films are presented in Fig. 1. The mono-layer film is found to be amorphous since a broad hump assigned to this layer and the underlying glass substrate is seen in the low 2θ region extending from 15 to 35° [13]. This fact may be explained by both the diffusion of atoms from glass substrate to the film and to the small amount of TiO₂. The bi-layer film shows a broad peak belonging to the anatase phase. As suggested by Shang et al. [14], the diffusion of glass into the TiO₂ layer is unavoidable during baking the sample in an oven at 500 °C, but with the increase in film thickness, this influence disappears. Thus, the effect of the diffusion of glass on crystallization is not so significant owing to the thicker TiO₂ film that covers the glass substrate and, at the same time, the increasing amount of TiO₂, which both result in the crystallization of the TiO₂ film. In the other work by Shinde et al. [15], the formation of the crystalline anatase phase is dependent on the film thickness.

The Raman spectra in Fig. 2 confirm the amorphous nature of the mono-layer film and crystalline nature of the bi-layer film. The spectrum of bi-layer film exhibits the bands at around 144 (E_g), 197 (E_g), 398 (B_{1g}), 520 (B_{1g}) and 639 (E_g) cm^{-1} which are assigned to TiO₂ anatase [16]. The weak band at 570 cm^{-1} is attributed to some species of the glass substrate.

3.2. Surface morphology

The AFM images of mono and bi-layer films annealed at 500 °C are illustrated in Fig. 3. It is seen that the surface of the mono-layer

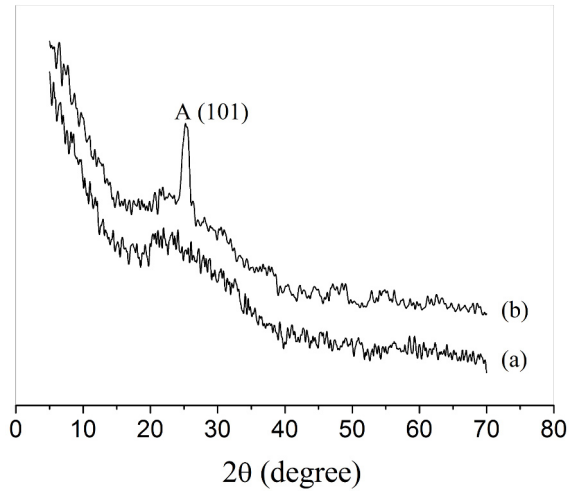


Fig. 1. X-Ray diffraction patterns of TiO₂ films: mono-layer (a) and bi-layer (b).

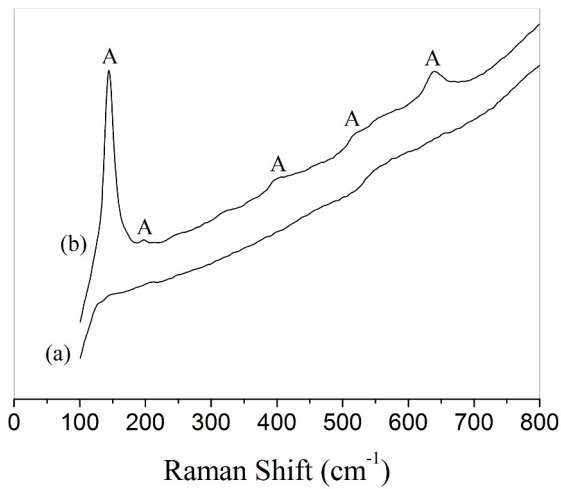


Fig. 2. The Raman spectra of TiO₂ thin films: mono-layer (a) and bi-layer (b).

film is relatively inhomogeneous, whereas that of bi-layer is more homogeneous on the whole area. The roughness parameter for the films has revealed a decrease with thickness. RMS values for mono-layer and bi-layer samples are 5.5 nm and 4 nm, respectively. In the other work, Euvananont et al. have also reported a decrease in RMS versus the thickness [17]. The surface roughness is a dominant factor which influences the optical properties.

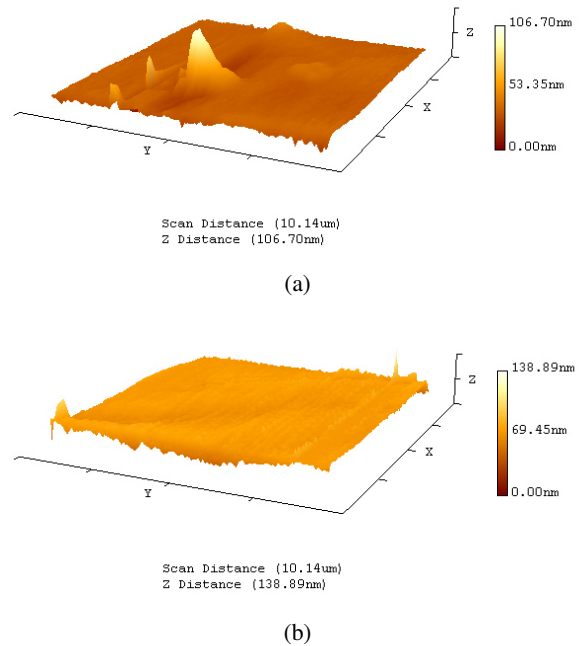


Fig. 3. AFM images of TiO₂ thin films: mono-layer (a) and bi-layer (b).

3.3. Optical properties

3.3.1. Ellipsometry measurements

The refractive index n and extinction coefficient k of mono and bi-layer films were calculated from SE measurements using the semi-infinite model in which the effect of the surface roughness was neglected. The values of n and k are given in Fig. 4 as a function of wavelength. The plotted curves of n and k are very similar to that described for the bulk [18]. In this figure, a similar tendency is observed for the curves of refractive index and extinction coefficient. These parameters gradually increase with the decrease of wavelength and sharply increase at the fundamental absorption edges where the wavelength threshold corresponds to the band gap of TiO₂ bulk crystal. The representative values of n at 550 and 633 nm wavelengths are given in Table 1. The increase in the film thickness causes an increase in the refractive index where the amorphous-to-anatase phase transition has been detected. The increase in the thickness indicates a structural modification so that the refractive index at 550 nm is relatively

close to that of TiO₂ anatase thin films prepared by sol-gel method [19, 20] and less than that of anatase bulk material [21]. It is important to say that the optical constants of TiO₂ films vary widely with a slight variation in the deposition conditions and also with the preparation method (chemical or physical method). In the work by Miao *et al.* [22], SE measurement results show that the films have higher refractive indexes than the values cited in the recent literatures, which gives an evidence for the compactness and fine crystallinity of the films deposited by sputtering method.

The behavior of refractive index is confirmed by the calculation of the film density using the well known Clausius-Mossotti relation [23]:

$$P = \left(\frac{n_f^2 - 1}{n_f^2 + 2} \right) \left(\frac{n_b^2 + 2}{n_b^2 - 1} \right) \quad (1)$$

where n_f and n_b are the refractive indices of the film and the bulk material of TiO₂, respectively. In the present study, n_b is taken as 2.57 [21]. It is clear that the packing density of the films increases with the increase in the thickness. We believe that fewer pores are left in TiO₂ thin films after volatilization of organic materials when the thickness increases. It is well known that in the sol-gel process, the organic products from the precursors would also influence the crystallinity as well as the optical properties of the films. The optical band gap E_g of TiO₂ films was determined using the extinction coefficient k [24]:

$$C(E - E_g) = \{(4\pi k/\lambda)h\nu\}^{\frac{1}{2}} \quad (2)$$

where C is a constant, $h\nu$ is the photon energy, $\alpha = 4\pi k/\lambda$ is the absorption coefficient at wavelength λ , k is the extinction coefficient.

An example of the plot of $(\alpha h\nu)^{\frac{1}{2}}$ versus photon energy of the films, including an extrapolation from the linear curve, is illustrated in Fig. 5. The mono-layer film has a high optical band gap of 3.42 eV. The bi-layer film, however, has anatase TiO₂ structure with the band gap of 3.29 eV. The evolution of the energy band gap, corresponding to previous research, is related to the crystallinity [25]. In this study, the decrease

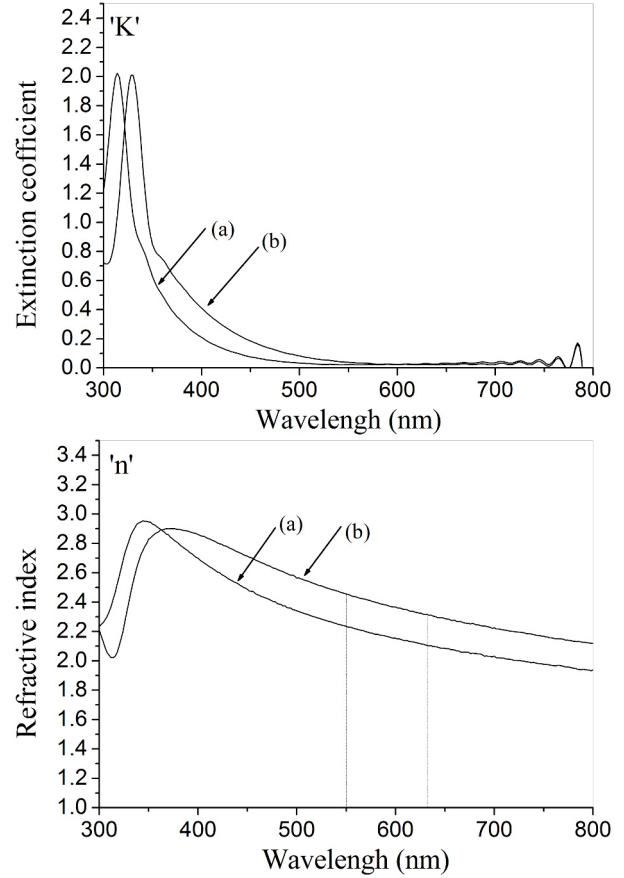


Fig. 4. Complex refractive index of TiO₂ films: mono-layer (a) and bi-layer (b), obtained from SE.

in the band gap is the result of the increase in thickness, which also induces crystallinity.

Table 1. Values of refractive indexes and packing density.

Samples	Refractive index (at 550 nm)	Refractive index (at 633 nm)	Packing density (at 550 nm)
Mono-layer	2.23	2.10	0.87
Bi-layer	2.45	2.30	0.95

3.3.2. Waveguiding measurements

The waveguiding properties of our films were investigated thanks to the m-lines spectroscopy [26]. It uses a prism coupling

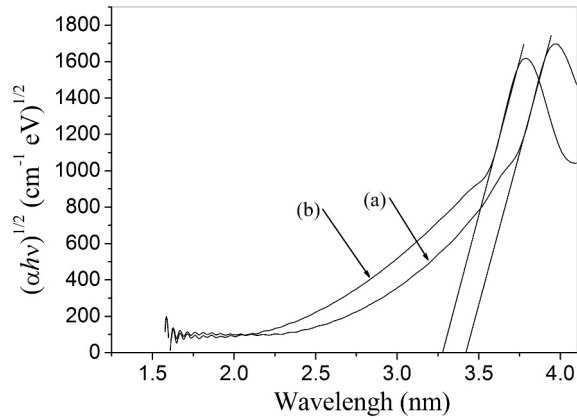


Fig. 5. Optical absorption spectra of TiO₂ films: mono-layer (a) and bi-layer (b) plotted as $(\alpha hv)^{1/2}$ versus hv .

method to launch the laser light into the optical layer. The intensity measured as a function of the incidence angle allows obtaining the mode profiles in the TE and TM polarisations. The measurements carried out on the bi-layer film in Fig. 6 display single-guided TE₀ and TM₀ polarized modes from which we can measure the refractive index and the film thickness using the TE/TM combination option. The results are reported in Table 2. With this approach, both films parameters (thickness and refractive index) are measured using the single TE₀ and TM₀ modes. The only requirement for this approach to be successful is that the film would not be birefringent, i.e., that the index of the film is isotropic. It is obvious that the value of refractive index obtained with this approximation is less than that obtained by SE measurements at 633 nm. In spite of this, the value of n obtained by m-lines spectroscopy agrees well with several literature values [27, 28]. In the sol-gel method, the values of n are always smaller than those of the bulk material, due to lower atomic densities of thin film material compared to bulk densities.

In other previous work, Mechiakh et al. [29] have reported the absence of TM modes in the TiO₂ thin films prepared from tetrabutyl-orthotitanate solution and butanol as a solvent by sol-gel dip coating technique. It was suggested that the lack of TM modes could be due to the crystallographic configuration and the surface roughness of the

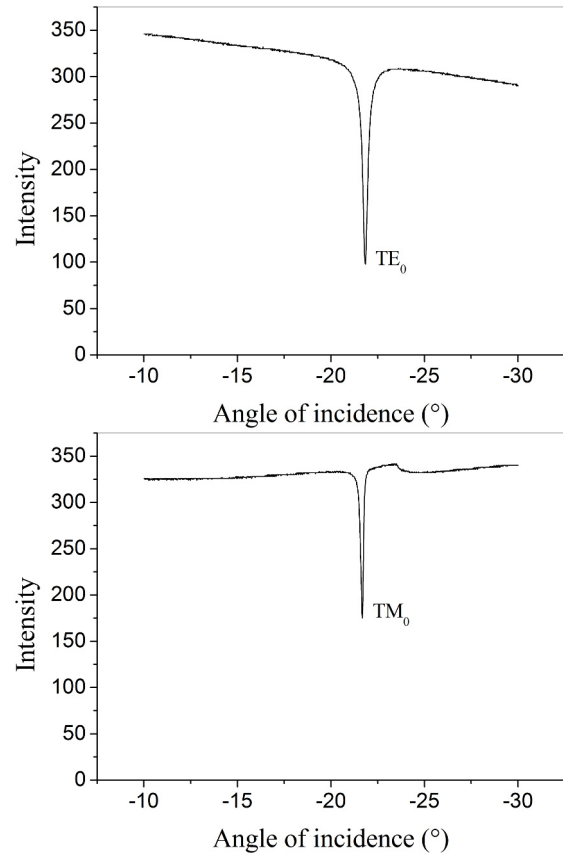


Fig. 6. Optical guided modes of the bi-layer TiO₂ thin film.

films. In our study, the sharpness of the dips is synonymous of a good confinement of the light into the guiding layer, which confirms that the sol-gel method is an interesting way to fabricate TiO₂ waveguides.

4. Conclusions

TiO₂ thin films have been prepared by sol-gel method on glass. The mono-layer film is amorphous but the bi-layer film consists of anatase phase oriented in the [101] direction. The Raman spectra confirm the XRD analysis. SE measurement results show that the refractive index increases with the film thickness. The value of refractive index of the bi-layer film at 633 nm obtained from SE is higher than that obtained by m-lines spectroscopy. Furthermore, the optical band gaps calculated by the extinction coefficient

Table 2. Measured values of opto-geometric parameters for bi-layer film.

Film thickness d (± 0.1 nm)	Effective index n (TE ₀) ($\pm 10^{-4}$)	Effective index n (TM ₀) ($\pm 10^{-4}$)	Refractive index ($\pm 10^{-4}$)
118.8	1.7311	1.5381	2.1282

from Tauc expression show that the bi-layer film has larger value than that of mono-layer. Explanation for this difference is ascribed to the increase in thickness, which also induces crystallinity. Waveguiding measurements carried out on bi-layer film show the excitation of single-guided TE₀ and TM₀ polarized modes.

References

- [1] LIN X., RONG F., JI X., FU D., *Micropor. Mesopor. Mat.*, 142 (2011), 276.
- [2] SHEN J., YANG T. H., ZHANG Q. Y., WANG J., ZHANG Q. Y., *J. Sol-Gel Sci. Techn.*, 26 (2003), 1029.
- [3] VERMA A., KAR M., AGNIHOTRY S. A., *Sol. Energ. Mat. Sol. C.*, 91 (2007), 1305.
- [4] ALJUFAIRI N. H., *Energy*, 39 (2011), 1.
- [5] WU Z. M., ZHANG W. Q., DONG C., *Vacuum*, 2 (2003), 19.
- [6] GARAPON C. et al., *Appl. Surf. Sci.*, 96–98 (1996), 836.
- [7] RODRIGUEZ R., JIMÉNEZ-SANDOVAL S., ESTEVEZ M., VARGAS S., *J. Non-Cryst. Solids*, 351 (2005), 167.
- [8] MALI S. S., SHINDE P. S., BETTY C. A., BHOSALE P. N., LEE W. J., PATIL P. S., *Appl. Surf. Sci.*, 257 (2011), 9737.
- [9] HUANG C. H., TSAO C. C., HSU C. Y., *Ceram. Int.*, 37 (2011), 2781.
- [10] FARKAS B., BUDAI J., KABALCI I., HESZLER P., GERETOVSKY ZS., *Appl. Surf. Sci.*, 254 (2008), 3484.
- [11] PARNA R., JOOST U., NOMMISTE E., KAAMBRE T., KIKAS A., KUUSIK I., HIRSIMAKI M., KINK I., KISAND V., *Appl. Surf. Sci.*, 257 (2011), 6897.
- [12] WELLIA D. V. et al., *Appl. Catal. A-Gen.*, 401 (2011), 98.
- [13] VERMA A., AGNIHOTRY S.A., *Electrochim. Acta*, 52 (2007), 2701.
- [14] SHANG J., YAO W., ZHU Y., WU N., *Appl. Catal. A-Gen.*, 257 (2004), 25.
- [15] SHINDE P. S. et al., *Sol. Energ. Mat. Sol. C.*, 92 (2008), 283.
- [16] MECHIAKH R., BEN SEDRINE N., BEN NACEUR J., CHTOUROU R., *Surf. Coat. Tech.*, 206 (2011), 243.
- [17] EUVANANONT C., JUNIN C., INPOR K., LIMTHONGKUL P., THANACHAYANONT C., *Ceram. Int.*, 34 (2008), 1067.
- [18] RIBALSKI M. W., *Handbook of Optical Constants of Solids I*, Academic Press, San Diego, 1998.
- [19] MECHIAKH R., BEN SEDRINE N., CHTOUROU R., *Appl. Surf. Sci.*, 257 (2011), 9103.
- [20] HAIMI E., LIPSONEN H., LARISMAA J., KAPULAINEN M., KRZAK-ROS J., HANNUL S.-P., *Thin Solid Films*, 519 (2011), 5882.
- [21] PALIK A., *Handbook of Optical Constants*, Academic, New York, 1985.
- [22] MIAO L., JIN P., KANEKO K., TERAJ A., NABATOVA-GABAIN N., TANEMURA S., *Appl. Surf. Sci.*, 212–213 (2003), 255.
- [23] SUBRAMANIAN M., VIJAYALAKSHMI S., VENKATARAJ S., JAYAVEL R., *Thin Solid Films*, 516 (2008), 3776.
- [24] TANEMURA S., MIAO L., JIN P., KANEKO K., TERAJ A., NABATOVA-GABAIN N., *Appl. Surf. Sci.*, 212–213 (2003), 654.
- [25] EIAMCHAI P., CHINDAUDOM P., POKAIPISIT A., LIMSUWAN P., *Curr. Appl. Phys.*, 9 (2008), 707.
- [26] ULRICH M., TORGE R., *Appl. Optics*, 12 (1973), 2901.
- [27] SREEMANY M. AND SEN S., *Mater. Chem. Phys.*, 83 (2004), 169.
- [28] MATHEWS N. R., MORALES E. R., CORTÉS-JACOME M. A., TOLEDO ANTONIO J. A., *Sol. Energy*, 83 (2009), 1499.
- [29] MECHIAKH R., MERICHE F., KREMER R., BENSABA R., BOUDINE B., BOUDRIOUA A., *Opt. Mater.*, 30 (2007), 645.

Received 2013-04-22
Accepted 2013-11-08